Mechanism of Alkene Rotation in Octahedral d^6 *trans*-Bis(alkene) Complexes of Molybdenum

Chen-Hsing Lai and Chien-Hong Cheng*

Department of Chemistry, National Tsing Hua University, Hsinchu, Taiwan 300, Republic of China

Received January 4, 1993®

Treatment of $Mo(CO)_4(NN)$ with 2 equiv of *N*-methylmaleimide in refluxing toluene led to the formation of $Mo(CO)_2(MeMI)_2(NN)$ (MeMI = *N*-methylmaleimido, NN = bpy (1), phen (2)). There are three possible rotamers **c-I**–**c-III** for a bis(maleimido) complex. To learn the exact conformation of the imide ligands, 1 was selected for X-ray structural analysis. This compound crystallizes in the monoclinic space group $C2/c$ with unit cell dimensions a = 16.612(4) Å, b = 14.187(3) Å, c = 13.759(4) Å, and β = 125.94(2)° with Z = 4; least-squares refinement based on 1794 independent observed reflections produced final R = 0.0235 and R_w = 0.0242. The results of X-ray structural analysis reveal 1 to be distorted octahedral with the two CO groups cis to each other, but each trans to a pyridyl group. The two MeMI are mutually orthogonal, and each MeMI ligand eclipses a N–Mo–CO vector. In addition, the central nitrogen atom of each MeMI ligand points to one carbonyl group. Thus, the conformation of 1 in the solid state is **c-I**. Variable-temperature NMR studies of $Mo(CO)_2(MeMI)_2(bpy)$ indicate that the complex in solution exists as a mixture of rotamers **c-I** and **c-II** that interchange rapidly above room temperature due to the rotation of the two alkene ligands. Several mechanisms of alkene rotation have been considered. From the NMR results of 1 and complexes $Mo(CO)_2(DMFU)_2(NN)$ (DMFU = dimethyl fumarato; NN = bpy and phen), we conclude that, in these octahedral *trans*-bis(alkene) complexes, alkene rotation takes place via a conrotatory mechanism. A dissociative process involving the exchange of free and coordinated alkenes and nondissociative mechanisms involving disrotatory motion and independent motion of the alkene ligands cannot account for all the observations.

Introduction

Octahedral d^6 *trans*-bis(alkene) and the related bis(η^2-ligand) complexes have attracted considerable attention about the mechanism of rotation and the conformation of these η^2 ligands.[1] Several octahedral d^6 *trans*-bis(ethylene) complexes of chromium, molybdenum, and tungsten have been reported,[2] and we have successfully prepared complexes $Mo(CO)_2(DMFU)_2(NN)$ (DMFU = dimethyl fumarato; NN = bidentate nitrogen ligand).[3] Due to the prochiral nature of DMFU, two diastereomers **a** and **b** of these bis(DMFU) complexes arising from the face selectivity of the ligand were isolated. For the bpy or phen complex, the diastereomer **a** exists as two rotamers **a-I** and **a-II** in thermodynamic equilibrium in solution. Both **a** and **b** are fluxional because of the rotation of the alkene ligands. The rotations of alkyne[4] and carbon dioxide[5] ligands in the corresponding *trans*-bis(η^2-ligand) complexes are known to follow a conrotatory process, but the mechanism of alkene rotation has not been investigated experimentally. Here, we report the synthesis and characterization of bis(MeMI) complexes (MeMI = *N*-methylmaleimido) which show unusual conformational preference and interesting dynamic NMR behavior of the imide ligands. These results and those of the bis(DMFU) complexes allow us to elucidate unequivocally the mechanism of alkene rotation in these bis(alkene) complexes.

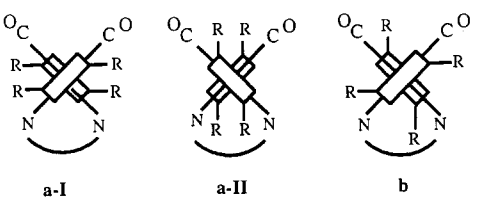

Results and Discussion

Treatment of $Mo(CO)_4(NN)$ with 2 equiv of *N*-methylmaleimide in refluxing toluene solution for 4 h led to the formation of $Mo(CO)_2(MeMI)_2(NN)$ (NN = bpy (1), phen (2)) in more than 90% yield. There are three possible rotamers **c-I**–**c-III** (Scheme I) for a bis(maleimido) complex. To learn the exact conformation of the imide ligands, 1 was selected for X-ray structural analysis. An ORTEP diagram of 1 with atomic numbering is shown in Figure 1; its atomic coordinates are listed in Table I, and

® Abstract published in *Advance ACS Abstracts*, August 15, 1993.

(1) (a) Bachmann, C.; Demuynck, J.; Veillard, A. *J. Am. Chem. Soc.* **1978**, *100*, 2366. (b) Marcos, E. S.; Caballol, R.; Trinquieer, G.; Bartherlat, J.-C. *J. Chem. Soc., Dalton Trans.* **1987**, 2373. (c) Alvarez, R.; Carmona, E.; Marin, J. M.; Poveda, M. L.; Gutierrez-Puebla, E.; Monge, A. *J. Am. Chem. Soc.* **1086**, *108*, 2286. (d) Chevrier, B.; Diebold, Th.; Weiss, R. *Inorg. Chim. Acta* **1976**, *19*, L57.

(2) (a) Carmona, E.; Marin, J. M.; Poveda, M. L.; Atwood, J. L.; Rogers, R. D. *J. Am. Chem. Soc.* **1983**, *105*, 3014. (b) Byrne, J. W.; Blaser, H. U.; Osborn, J. A. *J. Am. Chem. Soc.* **1975**, *97*, 3871. (c) Gregory, M. F.; Jackson, S. A.; Poliakoff, M.; Turner, J. J. *J. Chem. Soc., Chem. Commun.* **1986**, 1175. (d) Carmona, E.; Galindo, A.; Poveda, M. L.; Rogers, R. D. *Inorg. Chem.* **1985**, *24*, 4033. (e) Carmona, E.; Galindo, A.; Marin, J. M.; Gutierrez-Puebla, E.; Monge, A.; Ruiz, C. *Polyhedron* **1988**, *7*, 1831. (f) Grevels, F.-W.; Jacke, J.; Ozkar, S. *J. Am. Chem. Soc.* **1987**, *109*, 7536. (g) Hohmann, F.; Dieck, H. T.; Kruger, C.; Tsay, Y.-H. *J. Organomet. Chem.* **1979**, *171*, 353.

(3) Lai, C. H.; Cheng, C. H.; Chou, W. C.; Wang, S. L. *Organometallics* **1993**, *12*, 1105.

(4) (a) Hsiao, T. Y.; Kuo, P. L.; Lai, C. H.; Cheng, C. H.; Cheng, C. Y.; Wang, S. L. *Organometallics* **1993**, *12*, 1094. (b) Birdwhistll, K. R.; Tonker, T. L.; Templeton, J. L. *J. Am. Chem. Soc.* **1987**, *109*, 1401.

(5) Carmona, E.; Hughes, A. K.; Munoz, M. A.; O'Hare, D. M.; Perez, F. J.; Poveda, M. L. *J. Am. Chem. Soc.* **1991**, *113*, 9210.

0276-7333/93/2312-3561$04.00/0

Scheme I. Conrotatory Motion of Complexes 1 and 2

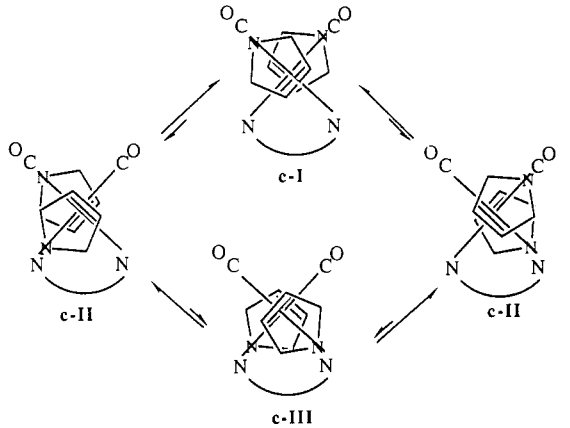

important intramolecular bond distances and bond angles are shown in Table II. These structural results show 1 to be distorted octahedral with the two CO groups cis to each other, but each trans to a pyridyl group. The two MeMI are mutually orthogonal (83.6°) and each alkene ligand eclipses a N–Mo–CO vector (171.7°). One interesting feature of this solid-state structure is that each imide molecule is oriented so that the central nitrogen atom points to one carbonyl group. The distance from the nitrogen atom to the carbonyl carbon is 2.903 Å, indicating weak bonding between the carbonyl carbon and the nitrogen atom.[6] The donation of the electron lone pair in the nitrogen atom to a π^* orbital of the carbonyl group likely accounts for the observed weak interaction. It is also possible that the observed solid conformation simply resulted from minimizing steric repulsion between the maleimide ligands and other moieties in the complex. Similar interligand interaction has been reported previously.[7]

It is interesting to see whether the structure of this complex in solution is the same as that in the solid state. Variable-temperature NMR studies of this species provide the answer to this question. The ^1H NMR spectrum in CD_2Cl_2 at 183 K indicates that the complex is static and two sets of signals corresponding to the presence of rotamers **c-I** and **c-II** in solution (Figure 2). The major set of resonances includes doublets at δ 4.02 and 2.24 for the olefin protons, a singlet at δ 2.76 for the methyl protons of the coordinated *N*-methylmaleimido, and four resonances in the aromatic region for the protons of the bpy ligand. Of the three possible rotamers, **c-II** is clearly eliminated as the rotamer associated with these major resonances based on the symmetry of the structure. Although both **c-I** and **c-III** are expected to have the same number of resonances, as is observed, we assign **c-I** as the major rotamer of complex 1 in solution in view of the results of the X-ray analysis. This proposed structure is further supported by the observed great difference, more than 1.5 ppm, in chemical shift of the two olefin protons.[8] The olefin proton at δ 2.27 is in the region between the two pyridyl grous, while the other at δ 4.08 lies in the region between the two carbonyl groups. Similar observations were found in the bis(DMFU) species.[3] The other set of signals with much weaker intensity at δ 4.51, 4.08, 3.84, and 2.16 for the olefin protons (all as doublets) is attributed

(6) Liu, L. K.; Sun, C. H.; Yang, C. Z.; Wen, Y. S.; Wu, G. F.; Shih, S. Y.; Lin, K. S. *Organometallics* **1992**, *11*, 972.
(7) Ball, R. G.; Burke, M. R.; Takats, J. *Organometallics* **1987**, *6*, 1918.
(8) Mayr, A.; Dorries, A. M.; Rheingold, A. L.; Geib, S. J. *Organometallics* **1990**, *9*, 964.

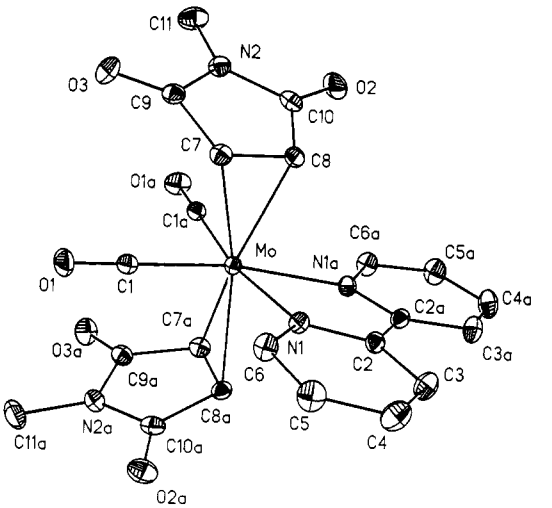

Figure 1. Molecular structure drawing of $Mo(CO)_2(MeMI)_2$-(bpy) (1) showing the atom-labeling scheme.

Table I. Atomic Coordinates ($\times 10^4$) and Equivalent Isotropic Displacement Coefficients ($Å^2 \times 10^3$) of 1

	x	*y*	*z*	*U*(eq)
Mo	0	18611(1)	2500	22(1)
C(1)	−888(3)	17622(3)	2403(3)	30(2)
C(2)	−504(3)	20733(3)	2365(3)	28(2)
C(3)	−994(3)	21554(3)	2273(4)	41(2)
C(4)	−1916(3)	21500(3)	2080(4)	49(2)
C(5)	−2316(3)	20624(3)	1970(4)	46(2)
C(6)	−1813(3)	19827(3)	2028(4)	37(2)
C(7)	−1241(3)	18287(3)	499(3)	31(2)
C(8)	−563(3)	18952(3)	591(3)	30(2)
C(9)	−1090(3)	18384(3)	97(3)	34(2)
C(10)	36(3)	18467(3)	279(3)	38(2)
C(11)	162(4)	16783(4)	−219(5)	55(3)
C(12)	−911(9)	14757(5)	1859(11)	134(10)
C(13)	−1759(7)	14183(8)	1353(8)	124(7)
O(1)	−1427(2)	17060(2)	2319(3)	47(2)
O(2)	714(2)	18752(2)	247(3)	53(2)
O(3)	−1522(2)	16642(2)	−125(3)	48(2)
O(4)	0	14232(4)	2500	68(4)
N(1)	−912(2)	19874(2)	2229(3)	28(1)
N(2)	−307(2)	17529(2)	−4(3)	35(2)

Table II. Important Bond Distances (Å) and Angles (deg) of 1

	Distances		
Mo–C(1)	1.983(5)	Mo–C(7)	2.319(3)
Mo–C(8)	2.263(4)	Mo–N(1)	2.231(3)
C(1)–O(1)	1.153(6)	C(7)–C(8)	1.417(6)
C(7)–C(9)	1.474(6)	C(8)–C(10)	1.466(8)
C(9)–N(2)	1.401(7)	C(10)–N(2)	1.410(5)
C(11)–N(2)	1.444(8)	C(9)–O(3)	1.209(5)
C(10)–O(2)	1.222(7)		
	Angles		
C(1)–Mo–C(7)	70.9(2)	C(1)–Mo–C(8)	106.8(1)
C(7)–Mo–C(8)	36.0(2)	C(1)–Mo–N(1)	98.7(2)
C(7)–Mo–N(1)	85.3(1)	C(8)–Mo–N(1)	81.8(1)
C(1)–Mo–C(1A)	89.9(3)	C(7)–Mo–C(1A)	92.7(1)
C(8)–Mo–C(1A)	90.8(2)	N(1)–Mo–C(1A)	169.9(2)
Mo–C(1)–O(1)	178.1(3)	Mo–C(7)–C(8)	69.9(2)
Mo–C(7)–C(9)	112.9(2)	Mo–C(8)–C(7)	74.1(3)

to rotamer **c-II** on the basis that all four olefin protons in this rotamer have different environments. The presence of **c-II** is further evidenced by the observation of eight minor signals in the aromatic region for the bpy ligand and a singlet at δ 1.75 for the methyl protons pointing toward a pyridyl ring. Due to the ring-current effect of bpy, the chemical shift of these methyl protons is more than 1 ppm upfield than that of **c-I**. From the peak intensities, the ratio of the relative populations of **c-I** and **c-II** was calculated to be 7:1 at 185 K. As the temperature

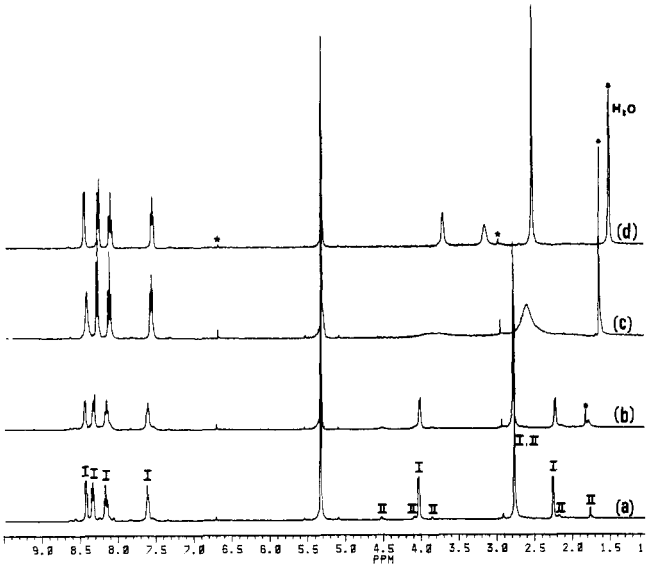

Figure 2. ^1H NMR spectrum of 1 (in CD_2Cl_2) at (a) 185 K, (b) 220 K, (c) 258 K, and (d) 313 K.

increased, interconversion between rotamers **c-I** and **c-II** become rapid and peak broadening was observed. At temperatures above 333 K (in $CDCl_3$), the fast-exchange limit was reached. The ^1H NMR spectrum displays two doublets at δ 3.69 and 3.51 for the olefin protons, one singlet at δ 2.51 for the methyl protons, and four signals in the aromatic region for the bpy ligand. Similar dynamic NMR behavior was observed for **2**. The ratio of relative populations of the rotamers **c-I** and **c-II** in **2** is 15:1 at 185 K.

Mechanism of Alkene Rotation. There is no ligand exchange observed between external alkenes and the coordinated alkene ligands under the conditions for dynamic NMR investigations. Thus, an intermolecular process involving dissociation–association of alkenes is ruled out for the dynamic behavior of bis(alkene) complexes. Three different intramolecular rotational processes are possible to account for the observed dynamic NMR behavior of bis(alkene) complexes: (i) disrotatory motion

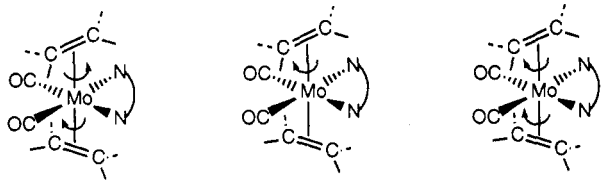

of the two coordinated alkenes; (ii) independent rotation of the alkene ligands; (iii) conrotatory motion of the two coordinated alkenes. We will carefully consider these three processes in order to determine the correct mechanism for alkene rotation.

The disrotatory mechanism accounts nicely for the interconversion between rotamers **a-I** and **a-II** of diastereomer **a** of complexes $Mo(CO)_2(DMFU)_2(NN)$ (NN = bpy and phen) but fails to explain the observed facile interconversion between rotamers **c-I** and **c-II** and the observation of two olefin proton signals for complex **1** in the fast-exchange regime (eq 1). According to this process, only one signal should be observed.

The independent rotation (mechanism II) process involves the rotation of a coordinated alkene by 90° to

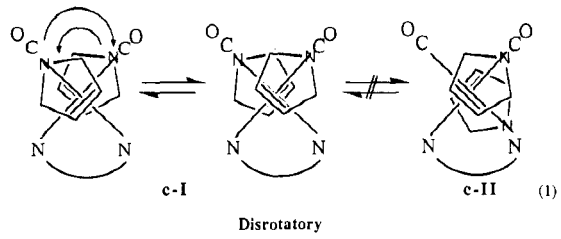

give intermediates or transition states such as **I**, followed by an independent rotation of either of the two eclipsed

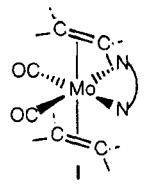

I

alkenes by 90°. The intermediate **I** introduces an effective plane of symmetry and renders equivalent the two DMFU ligands. This process successfully explains the NMR behavior of the diastereomers **a** and **b** of $Mo(CO)_2(DMFU)_2(NN)$ (NN = bpy or phen). However, it predicts a single resonance for the olefin protons and carbons on the MeMI ligands of complex **1** in the fast-exchange limit in contrast to the observed NMR spectra. On this basis, the mechanism can be disregarded.

For the mechanism of conrotatory motion, the two trans alkenes rotate synchronously in the same direction and remain mutually orthogonal during the rotation. A transition state or an intermediate such as **II** is expected

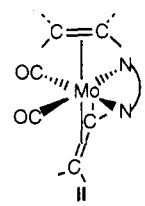

II

to be involved in this intramolecular process. It is the only mechanism that can account for all observations for the fluxional NMR behavior of $Mo(CO)_2(DMFU)_2(NN)$ and $Mo(CO)_2(MeMI)_2(NN)$. As shown in Scheme I, the process successfully explains the interconversion of rotamers **c-I** and **c-II** of complex **1**. In accordance with the NMR results, the mechanism predicts two olefin proton and two olefin and two keto carbon-13 signals for complex **1** even in the fast-exchange regime. This process leads neither to interchange of two olefin carbons nor to proton interchange in each maleimido ligand. Application of this pathway to the rotation of DMFU on diastereomers **a** (Scheme II) and **b** of $Mo(CO)_2(DMFU)_2(NN)$ (NN = bpy or phen) successfully accounts for the dynamic NMR behavior of these species. Therefore, we conclude that, in octahedral *trans*-bis(alkene) complexes, alkene rotation takes place synchronously in the same direction. For **1** and **2**, the MeMI ligands' swinging back and forth among the three positions shown in rotamers **c-I** and **c-II** (Scheme I) is expected to be the main pathway of alkene rotation. The rotation from **c-II** to **c-III** is much less probable in view of the absence of **c-III** in the NMR spectra of complex **1**. Thus, each MeMI mainly rotates within a range of 180°. For the bis(DMFU) complexes (Scheme II), the two DMFU ligands show no such limitation of angle for the rotation. It is interesting to note that the present mechanistic conclusion contradicts previous theoretical

Scheme II. Conrotatory Motion of Diastereomer a of $Mo(CO)_2(DMFU)_2(NN)$ Where NN = bpy or phen

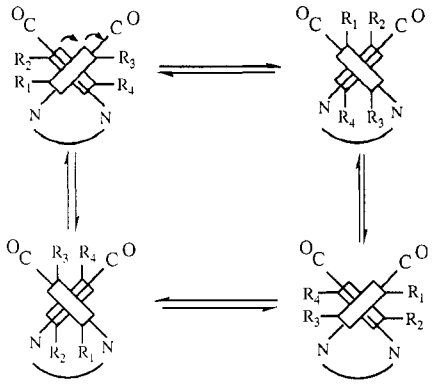

results, which indicated that independent rotation slightly favors conrotatory motion,[1a] but is similar to the experimental conclusions for the bis(alkyne)[4] and for bis(carbon dioxide)[5] complexes.

Experimental Section

All experiments were performed under dry nitrogen, and all solvents were purified under N_2 by standard methods. ^1H and ^{13}C NMR spectra were recorded on Bruker AM-400 and Varian Gemini-300 instruments; infrared spectra were measured on a Bomem MB-100 spectrometer. Elemental analyses were performed by Heraeus CHN-O-RAPID. All reagents were used as obtained from commercial sources. For X-ray structure determination a Siemens R3m/V diffractometer was used.

2,2′-Bipyridine, 1,10-phenanthroline (Merck), *N*-methylmaleimide (Janssen), and molybdenum hexacarbonyl (Strem) were used as received. $Mo(CO)_4$(bpy) and $Mo(CO)_4$(phen) were prepared according to reported methods.[9]

Synthesis of $Mo(CO)_2$(bpy)(*N*-methylmaleimido)$_2$ (1). A mixture of $Mo(CO)_4$(bpy) (0.300 g, 0.824 mmol) and *N*-methylmaleimide (0.230 g, 2.06 mmol) in toluene (10 mL) was refluxed for 4 h. An orange precipitate was obtained as the reaction mixture was cooled to room temperature. Recrystallization from a mixture of CH_2Cl_2/Et_2O gave the desired product 1 (0.40 g) as orange crystalline material in 93% yield. ^1H NMR (CD_2Cl_2, 294 K): δ 8.45 (d, J = 5.2 Hz, 2 H, H-3,3′ of bpy), 8.29 (d, J = 8.1 Hz, 2 H, H-6,6′ of bpy), 8.13 (dd, J = 8.1 Hz, J = 7.9 Hz, 2 H, H-5,5′ of bpy), 7.57 (dd, J = 7.9 Hz, J = 5.2 Hz, 2 H, H-4,4′ of bpy), 3.75 (b, 2 H, =CH), 3.02 (b, 2 H, =CH), 2.58 (s, 6 H, N—CH_3). $^{13}C\{^1H\}$ NMR (CD_2Cl_2): δ 220.32 (C≡O), 177.48, 177.06 (C=O), 153.30, 152.81, 139.48, 127.05, 123.77 (bpy), 62.63, 60.92 (=CH), 22.88 (CH_3). IR (KBr): 1955, 1888 (ν(C≡O)), 1723, 1666 (ν(C=O)). Anal. Calcd for $MoC_{22}H_{18}N_4O_6 \cdot C_4H_{10}O$: C, 51.66; H, 4.64; N, 9.27. Found: C, 51.28; H, 4.60; N, 9.38.

$Mo(CO)_2$(phen)(*N*-methylmaleimido)$_2$ (2). The title compound was prepared in 92% yield following a procedure similar to that described for 1. ^1H NMR (CD_2Cl_2, 294 K): δ 8.83 (dd, J = 5.1 Hz, J = 1.2 Hz, 2 H, H-2,9 of phen), 8.61 (dd, J = 8.2 Hz, J = 1.6 Hz, 2 H, H-4,7 of phen), 8.08 (s, 2 H, H-5,6 of phen), 7.89 (dd, J = 5.1 Hz, J = 8.2 Hz, 2 H, H-3,8 of phen), 3.88 (b, 2 H, =CH), 2.63 (b, 8 H, =CH, N—CH_3). $^{13}C\{^1H\}$ NMR (CD_2Cl_2): δ 220.28 (C≡O), 177.76, 177.18 (C=O), 152.90, 144.28, 138.68, 131.28, 128.25, 125.78 (phen), 62.79, 60.02 (C=C), 22.96 (CH_3). ^1H NMR (CD_2Cl_2, 173 K): δ 8.79 (d, J = 4.8 Hz, 2 H, H-2,9 of phen), 8.65 (d, J = 7.9 Hz, 2 H, H-4,7 of phen), 8.10 (s, 2 H, H-5,6 of phen), 7.91 (dd, J = 4.8 Hz, J = 7.9 Hz, 2 H, H-3,8 of phen), 4.10 (d, J = 5.5 Hz, 2 H, =CH), 2.76 (s, 6 H, N—CH_3), 2.10 (d, J = 5.5 Hz, 2 H, =CH). IR (KBr): 1969, 1901 (ν(C≡O)), 1728, 1673 (ν(C=O)). Anal. Calcd for $MoC_{24}H_{18}N_4O_6 \cdot H_2O$: C, 50.35; H, 3.50; N, 9.79. Found: C, 50.11; H, 3.52; N, 9.65.

X-ray Structure Determination of $Mo(CO)_2$(bpy)(MeMI) (1). An orange crystal of dimensions 0.20 × 0.21 × 0.36 mm^3 was selected for X-ray diffraction measurement. Data were collected on a Siemens R3m/V diffractometer equipped with a graphite-monochromated Mo source (Kα radiation, 0.7107 Å). Cell parameters as listed in Table III were determined from the fit of 15 reflections ($9.52 \le 2\theta \le 22.82°$). No significant variation in intensities of three standards monitored every 50 reflections occurred. A total of 3107 reflections were collected, but only 1794 unique reflections with $I \ge 3\sigma(I)$ were used for structure solution and refinement. These data were corrected for absorption, Lorentz, and polarization effects. Correction for absorption was based on ϕ scans of a few suitable reflections with χ values near 90° (T_{min}, T_{max} = 0.788, 0.910; μ = 5.52 cm^{-1}). Systematic absences were (hkl, $h + k = 2n + 1$; $h0l$, $h,l = 2n + 1$). The structure was solved using the Patterson-superposition technique and refined by a full-matrix least-squares method based on F values. The final residuals for variables and independent reflections with $I \ge 3\sigma(I)$ were R = 0.0337, R_w = 0.0361. The final difference Fourier map had no peak greater than 0.61 e Å^{-3}. The final positional parameters were determined with final refinements of the structure with Rogers' η value. Scattering factors were taken from *International Tables for X-ray Crystallography* (1974). All calculations were performed on a Micro VAX II computer system using SHELXTL-Plus programs.

Table III. Summary of Crystal Data and Data Collection of Compound 1

empirical formula	$C_{26}H_{28}MoN_4O_7$
color; habit	orange; chunk
cryst size, mm^3	0.20 × 0.21 × 0.36
space group	monoclinic; $C2/c$
unit cell dimens	
a, Å	16.612(4)
b, Å	14.187(3)
c, Å	13.759(4)
β, deg	125.94(2)
vol, Å^3	2625.1(11)
Z	4
fw	604.5
den (calc), g cm^{-3}	1.529
abs coeff, mm^{-1}	0.552
F(000)	1240
diffractometer used	Siemens R3m/V
radiation	Mo Kα (λ = 0.710 73 Å)
temp, K	296
2θ range, deg	2.5–50.0
scan type	$\theta/2\theta$
scan speed, deg min^{-1}	varible; 2.93–14.65 in ω
scan range (ω), deg	1.00 plus Kα separation
standard reflns	3 measd every 50 reflns
index ranges	$-19 \le h \le 16$, $0 \le k \le 16$, $-0 \le l \le 16$
no. of reflns collcd	3107 ($1910 \ge 3.0\sigma(I)$)
no. of ind reflns	2329 ($1794 \ge 3.0\sigma(I)$)
T_{min}/T_{max}	0.788/0.910
weighting scheme	$w^{-1} = \sigma^2(F) + 0.0018F^2$
no. of params refined	216
goodness of fit	0.84
final R indices (obs data)	R = 0.0235, R_w = 0.0242
largest and mean Δ/σ	0.001, 0.000
data-to-param ratio	10.3:1
largest diff peak/hol, e Å^{-3}	+0.61/−0.42

Acknowledgment. We thank the National Science Council of the Republic of China (NSC 81-0228-M-007-72) for support of this research.

Supplementary Material Available: Tables of crystal data, atomic positional parameters, complete bond distances and angles, thermal parameters, and hydrogen positions for 1 (4 pages). Ordering information is given on any current masthead page.

OM930002A

(9) Stiddard, M. H. B. *J. Chem. Soc.* **1962**, 4712.